International Journal of Biological Macromolecules 193 (2021) 441–449

Contents lists available at ScienceDirect

International Journal of Biological Macromolecules

journal homepage: www.elsevier.com/locate/ijbiomac

Cas12c-DETECTOR: A specific and sensitive Cas12c-based DNA detection platform

Zupeng Wang, Caihong Zhong *

Key Laboratory of Plant Germplasm Enhancement and Specialty Agriculture, Wuhan Botanical Garden, Chinese Academy of Sciences, Wuhan 430074, China
Innovative Academy of Seed Design, Chinese Academy of Sciences, Beijing 100101, China
Engineering Laboratory for Kiwifruit Industrial Technology, Chinese Academy of Sciences, Wuhan 430074, China

ARTICLE INFO

Keywords:
Cas12c
CRISPR
Nucleic acid detection
Sensitivity
SNP

ABSTRACT

The robust and precise nucleic acid detection platform enormously influences the clinical diagnosis of human and plant pathogens, drastically affecting disease pandemic control. CRISPR-based nucleic acid detection tools have been successfully applied for rapid and sensitive nucleic acid detection. However, the T-rich protospacer adjacent motif (PAM), specificity, and sensitivity of the CRISPR-based nucleic acid detection tools limited its wide application. We first developed a new Cas12c-based nucleic acid detection platform (Cas12c-DETECTOR), recognizing a 5′-TG PAM and showing high sensitivity and specificity on examined targets. Our results indicate that Cas12c-DETECTOR coupling with the optimized single-guide RNA (sgRNA) can be applied to specifically identity single nucleotide polymorphism (SNP). Moreover, combined with pre-amplification and lateral flow strips or the visual fluorescence detection method, Cas12c-DETECTOR can be used to diagnose human and plant pathogens in practice. Therefore, our findings illustrated that Cas12c-DETECTOR is a robust, sensitive, precise, and practiced nucleic acid detection platform.

1. Introduction

The prokaryotic clustered regularly interspaced short palindromic repeat (CRISPR) and CRISPR-associated protein (CRISPR/Cas) system is the immune system of bacterium and archaea, playing a critical role in the competition between bacterium and virus [1]. Class 2 CRISPR/Cas systems have been characterized and employed for targeted genome modification and nucleic acid detection based on their programmable single-effector nucleases [2,3]. According to the properties of their single-effector nucleases, class 2 CRISPR/Cas systems can be divided into three types (types II, V, and VI) [2]. The single-effector nuclease of type II CRISPR/Cas system (Cas9) harbors two nuclease domains (the HNH and RuvC nuclease domains), and the two nuclease domains are responsible for the cleavage of the double-strand DNA (dsDNA) [4]. In contrast, the single-effector nuclease of type V (Cas12) contains a single RuvC nuclease domain corresponding to the cleavage of dsDNA and single-strand DNA (ssDNA) [4]. The single-effector nuclease Cas13 and Cas14 of type VI conclude two HEPN domains that induce the targeted RNA degradation [5].

Sensitive and precise nucleic acid detection platforms are critical for the clinical diagnosis of pathogenic microorganisms, genotyping, and plant-pathogen detection [5]. CRISPR/Cas-based nucleic acid detection platforms have been developed and based on the Cas protein; CRISPR/Cas-based nucleic acid detection platforms are classified into four types (Cas9-, Cas12-, Cas13-, and Cas14-based nucleic acid detection platforms) [6,7]. Cas9-based nucleic acid detection can be classified into three categories based on Cas9 variants. The Cas9-based nucleic acid detection employs the RNA-guided DNA cleavage of Cas9 coupling with extra steps, and four Cas9-based nucleic acid detection tools are developed, including NASBACC [8], NASBACC CAS-EXPAR [9], RACE [10], and CASLFA [11]. The second subtype is the dCas9-based nucleic acid detection platform, which utilizes the RNA-guided DNA binding activity of dCas9 and five dCas9-based nucleic acid detection tools have been developed, including dCas9/sgRNA-SG I based MRSA detection [12], PC reporter [13], RCH [13], CRISPR–Chip [14], and Nanoelectrokinetic platform [15]. The third type is the Cas9n-based nucleic acid detection platform, which employs RNA-guided DNA nicking activity of Cas9n, and two Cas9n-based nucleic acid detection tools have been developed, including CRISDA [16] and Cas9nAR [17]. However, Cas9-based nucleic acid detection platforms require additional complicated steps to perform

* Corresponding author at: Key Laboratory of Plant Germplasm Enhancement and Specialty Agriculture, Wuhan Botanical Garden, Chinese Academy of Sciences, Wuhan 430074, China.
E-mail addresses: wangzupeng@wbgcas.cn (Z. Wang), zhongch@wbgcas.cn (C. Zhong).

https://doi.org/10.1016/j.ijbiomac.2021.10.167
Received 30 August 2021; Received in revised form 21 October 2021; Accepted 22 October 2021
Available online 26 October 2021
0141-8130/© 2021 Elsevier B.V. All rights reserved.

nucleic acid detection [6]. The Cas13-based nucleic acid detection platforms were developed based on RNA-guided target-recognition-triggered collateral single-strand RNA cleavage of Cas13 protein, and Cas13a- and Cas13b-based nucleic acid detection tools have been established [5,18]. The Cas13-based nucleic acid detection platform (referred to as SHERLOCK) has been applied for detections of RNA viruses, like Zika virus (ZIKA) and dengue virus (DENV), and SNP identifications in human cells [5,19]. The Cas13 only targets single-strand RNA (ssRNA), and the SHERLOCK also needs the additional T7 in vitro transcription process to detect DNA, which increases its complexity [19]. The Cas14-based nucleic acid detection platform utilizes target recognition-triggered nonspecific cutting of ssDNA molecules of Cas14 [20]. The Cas14-based DETECTR was successfully used for single nucleotide polymorphism (SNP) identification in the *HERC2* gene [20]. However, the Cas14 only binds and cleaves ssDNA, which needs another step to form ssDNA from double-strand DNA and impedes its application [20].

The Cas12-based nucleic acid detection platforms can detect dsDNA by utilizing their capability to cleave the *trans*-cleave ssDNA reporter, and Cas12a- and Cas12b-based nucleic acid detection platforms have been successfully applied for nucleic acid detection [21–23]. Notably, Cas12a-based detectors have been used to detect the betacoronavirus rapidly, which causes severe acute respiratory syndrome (SARS)-CoV-2 (CoVID2019) [24]. However, both Cas12a- and Cas12b-based nucleic acid detection platforms need a T-rich protospacer adjacent motif (PAM), and their specificity and sensitivity also need to be improved, affecting its applications [23]. Although the previous Cas-based nucleic acid detection platforms can sensitively and specifically detect RNA or DNA, they still need further improvement, and new platforms with prominent features are still desired.

Although subtype V-A (Cas12a) and V—B (Cas12b) have been characterized in detail and reprogrammed for targeted genome modification and nucleic acid detection [22,23], uncharacterized subtypes of type V Cas protein have distinct domain architectures and diverged RuvC sequences compared to Cas12a and Cas12b indicating potential unexplored properties and functional diversity [4]. The subtypes V—C (Cas12c) and V—D (Cas12d) have been identified and have the highest sequence similarity among different subtypes of type V [4,25]. Previous

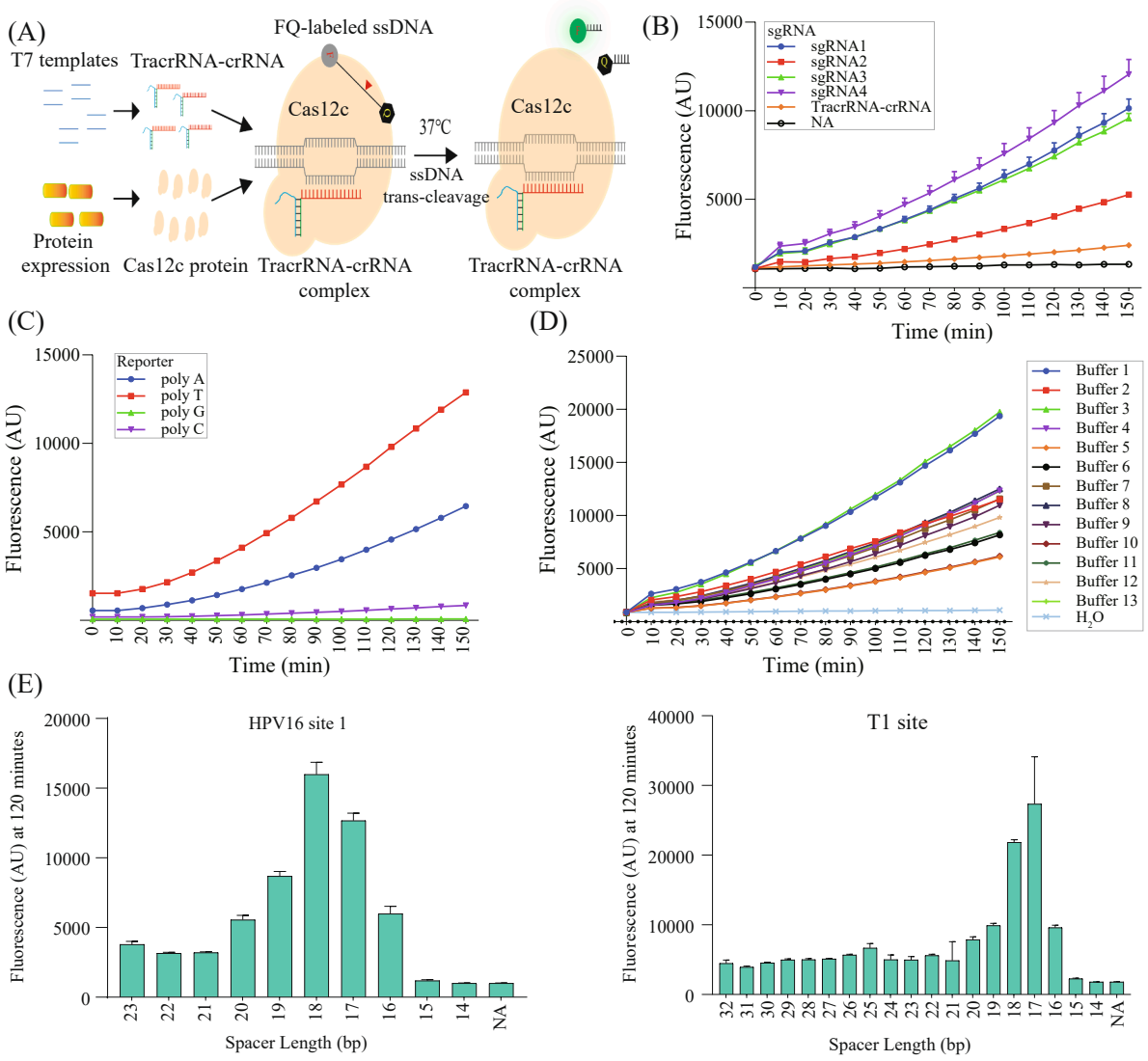


Fig. 1. Estimation and optimization for the *trans*-cleavage activity of Cas12c1. (A) The illumination of the *trans*-cleavage activity of Cas12c1 and the FQ-labeled reporter array. (B) Optimization of the sgRNA structure for Cas12c1. Error bars indicate standard errors of the mean (s.e.m.)., n = 3. NA, no-sgRNA. (C) Base preference of Cas12c1-based *trans*-cleavage of ssDNA reporters containing a homopolymer of A, T, G, or C bases. The T1 target was used in this test. Error bars indicate standard errors of the mean (s.e.m.), n = 3. (D) Buffer optimization of Cas12c1 *trans*-cleavage activity. (E) Effect of the spacer length on the Cas12c1 *trans*-cleavage activity. Error bars indicate standard errors of the mean (s.e.m.)., n = 3. NA, no-sgRNA.

results indicate that Cas12c and Cas12d facilitate RNA-guided DNA interference in the bacteria [4,25]. However, the RNA-guided DNA interference activity of Cas12c and Cas12d cannot be reconstructed in vitro using the CRISPR RNA (crRNA) [4,26]. Recently, the RNA-guided DNA interference activity of Cas12d is reconstructed in vitro using the short-complementarity untranslated RNA (scoutRNA) and the crRNA, and its *trans*-ssDNA cleavage activity has been verified that can be employed for nucleic acid detection [25]. Unfortunately, the RNA-guided DNA cleavage and *trans*-ssDNA cleavage activities of Cas12c have not been verified using the same method employed by Cas12d [4,25].

Based on the close phylogenetic relationship, we hypothesized that Cas12c might also have the ssDNA *trans*-cleavage activity, which could be utilized to develop the new nucleic acid detection platform [2,25]. Three Cas12c, including Cas12c1, Cas12c2, and OspCas12c, have been reported with different PAMs [4]. Cas12c1 and OspCas12c have a 5′ TG PAM, and Cas12c2 has a 5′ TN PAM, different from Cas12a and Cas12b [4,23]. In this study, we first validated that Cas12c1 possessed the ssDNA *trans*-cleavage activity (Fig. 1). Then, we developed and optimized the Cas12c-based nucleic acid detection platform (Cas12c-DETECTOR) and successfully applied it for virus detection (including human papillomavirus and CoVID2019) SNP identification, and plant pathogen detection. Furthermore, our results suggested that Cas12c-DETECTOR was a robust, sensitive, precise, and practical nucleic acid detection platform.

2. Material and methods

2.1. Protein expression and purification of Cas12c1 and Cas12a

For protein expression and purification, the plant codon-optimized Cas12c1 and LbCas12a genes were cloned into the bacterial expression vector pET-32a(+) and verified their sequences using Sanger sequencing (termed as pET-32a-Cas12c1 and pET-32a-LbCas12a). The Cas12c1 and LbCas12a expression vector was transformed into the Transetta (DE3) Chemically Competent Cell (Transgen). About 5 ml culture was grown overnight in 2xYT media at 37 °C and 200 rpm/min, which was incubated in 500 ml 2xYT media for growth at 37 °C and 200 rpm/min until the OD600 reached 0.6. Then protein expression was induced with 0.5 mM IPTG at 16 °C and 180 rpm/min for 16 h. Cells were centrifuged at 8000*g* for 3 min and stored at −80 °C for later protein purification. All the subsequent procedures were conducted at 4 °C. The cell pellet was resuspended in 30 ml cell lysis buffer (20 mM Phosphate Buffer, 500 mM NaCl, 10 mM Imidazole, pH = 7.4) supplemented with 50 μg/ml lysozyme and 1 mM protease inhibitors and disrupted by sonication for 10 mins (2 s pulse followed 2 s pause). Then lysate was cleared by centrifugation for 40 min at 4 °C and 8000 g. The protein purification was conducted using the His-tag Protein Purification Beads kit (SolarBio). Purified Cas12c1 and LbCas12a proteins were dialyzed, concentrated, and finally quantitated using the BCA Protein Assay Kit (Thermo Fisher).

2.2. Generation of sgRNAs for Cas12 proteins and dsDNA targets

The tracrRNA and direct repeats (DR) of Cas12c1 were synthesized by TsingKe Biotechnology Co., Ltd. (Table S5). The four sgRNA scaffolds were amplified from the tracrRNA using the corresponding primers (Table S4) and cloned into the pEASY-Blunt Zero Cloning vector forming psgRNA series (from psgRNA1 to psgRNA4) (Transgen). The crRNAs used for the Cas12a-based tool were synthesized according to the previous research [21].

The dsDNA activators of T1, HPV16 fragment, HPV18 fragment, CoVID2019 N gene fragment, CoVID2019 E gene fragment, SARS/Bat N gene fragment, and SARS/Bat E gene fragment were synthesized and cloned into the pEASY-Blunt Zero Cloning vector (Transgen) (Table S3). The dsDNA activators used for Cas12c detection arrays were amplified from positive clones using M13F/M13R primer pairs. The dsDNA activators of the *HopZ5* gene were amplified from the genomic DNA of Psa using the corresponding primers (Table S4) and purified using HiPure Gel Pure Micro Kit (Magen).

2.3. Transcription of tracrRNA, crRNA, and sgRNAs

The tracrRNA, crRNA, and sgRNAs were transcribed in vitro with T7 polymerase overnight at 37 °C using the HiScribe T7 Quick High Yield RNA Synthesis Kit (NEB), and the RNA was purified using MicroElute RNA Clean Up Kit (Omega). The T7 transcription templates (Table S5) were amplified from sgRNA scaffolds using the corresponding primers (Table S4) and purified using HiPure Gel Pure Micro Kit (Magen).

2.4. Fluorophore quencher (FQ)-labeled reporter assays

Homopolymer ssDNA FQ reporters (quenched fluorescent DNA reporter FAM-polyN5-BHQ1) were commercially synthesized by TsingKe Biotechnology Co., Ltd. (Table S4). The Cas12c detection arrays were performed with 50 nM Cas12c1, 40 nM sgRNA or tracrRNA-crRNA complex, 5 nM dsDNA activator, 200 nM homopolymer ssDNA FQ reporter and reaction buffer in a 20-μl reaction. The Cas12a detection arrays were conducted according to the procedures of the previous study [21]. Reactions (20 μl, 384-well microplate format) were incubated in a fluorescence plate reader (Tecan Infinite Pro F200) at 37 °C with fluorescence measurements taken every 10 min (λex = 485 nm; λem = 528 nm). Each experiment was conducted with three replicates. The fluorescence results were analyzed by GraphPad 8 software.

2.5. Optimizations for the Cas12c-DETECTOR

To optimize the sgRNA structure of Cas12c1, we designed four sgRNA structures (sgRNA1-sgRNA4) to replace the tracrRNA-crRNA complex (Fig. S1). We used the T1 dsDNA activator to conduct FQ-labeled reporter arrays to decide the best sgRNA structure. We performed FQ-labeled reporter arrays using four homopolymeric ssDNA reporters to evaluate the preferences of Cas12c1 on different homopolymeric ssDNA reporters (Table S1). Next, we optimized the reaction buffer of Cas12c1 by conducting FQ-labeled reporter arrays in 13 different buffers and used the ddH_2O setting as the control (Table S2). Further, we evaluated the effect of spacer lengths on the *trans*-cleavage activity of Cas12c1 using the HPV16-T1 (ranging from 14 to 23 bp) and T1 (ranging from 14 to 32 bp) targets with different sgRNA lengths (Table S6). We also used the HPV16-T1 and T1 targets to estimate the sensitivity and specificity of Cas12c-DETECTOR by setting a series of activator concentrations and mismatches in the spacer, respectively (Table S6).

2.6. Recombinase polymerase amplification (RPA) arrays

Genomic DNA was extracted from the healthy and diseased leaves of kiwifruit (*Actinidia chinensis*) using the filter paper-based DNA extraction method, according to Zou et al. (9). Next, We designed *HopZ5*-specific RPA primers using Primer3 software (http://bioinfo.ut.ee/primer3/). The RPA reaction was conducted using the TwistAmp Basic Kit (TwistDx) according to the instructions. The 50-μl RPA reaction system contained varying amounts of genomic DNA, 2.4 μl of forward and reverse primers (10 μM), 29.5 μl of rehydration buffer, and varying amounts of nuclease-free H_2O. The RPA reaction was incubated at 37 °C for 15 min. Then, two microlitres of the RPA products were added to the FQ-labeled reporter array.

2.7. Visible detection of the Cas12c-DETECTOR

We synthesized a new ssDNA reporter FQ5 (quenched fluorescent DNA reporter FAM-TTTTT-Biotin) used for the Cas12c-lateral flow strip

array (Cas12c-LFS) (Table S4). We next performed the Cas12c-DETECTOR reaction according to the FQ-reporter array using the FQ5 reporter. The reaction product of Cas12c-DETECTOR was diluted by adding an 80 μl phosphate buffer solution (PBS). A lateral flow strip (gendx) was then dipped in the reaction for 3 min, and the presentation of the control line and/or test line indicates the positive or negative result. For the visual fluorescence detection (VFD) of Cas12c, the reaction was set according to the FQ-labeled reporter array, and bright green fluorescence can be eradicated from the reaction products under blue light and observed using the yellow filter or a Blue Light Gel Imager (Sangon Biotech. Inc).

2.8. Validation of Cas12c-DETECTOR using contrived samples of CoVID2019

The nasopharyngeal swabs were collected from healthy persons previously informed and agreed. We simulated clinical samples by adding the pseudovirus (purchased from Yeasen Biotech) into the nasopharyngeal samples. The factitious samples were processed using MolPure® Viral DNA/RNA Kit (Yeasen Biotech). The pre-amplification of the N and E gene fragments was conducted using loop-mediated amplification (RT-LAMP) according to the procedure described by New England Biolabs (www.neb.com/protocols/2014/10/09/typical-rt-lamp-protocol) with a MgSO4 the concentration of 6.5 mM and a total volume of 10 μl.

2.9. Statistical analysis

All the experiments in this study consisted of three repeats. Uncertainties in the reported mean values were indicated as standard errors of the mean (s.e.m.). Statistical analysis was achieved using Graphpad Prism 8.

3. Results

3.1. Evaluation and optimization for the trans-cleavage activity of Cas12c

To test the collateral nonspecific ssDNA *trans*-cleavage activity of Cas12c, the codon-optimized Cas12c1 gene was synthesized and cloned into the bacterial expression vector pET-32a(+), and the corresponding protein was purified. The FQ-labeled reporter experiments have been widely employed for evaluating the ssDNA *trans*-cleavage activity of the Cas protein (Chen et al., 2018; Li et al., 2018; Teng et al., 2019). We also employed the FQ-labeled reporter array to estimate the ssDNA *trans*-cleavage activity of Cas12c1 (Fig. 1A). With the presentation of targeted dsDNA (referred to as activator), additions of complex tracrRNA and crRNA induced enhanced the fluorescence density compared to the control without tracrRNA-crRNA complex and sgRNA ($p\text{-value} < 0.01$), indicating that Cas12c1-tracrRNA-crRNA complex could *trans*-cleave the ssDNA reporter (Fig. 1B). To simplify the Cas12c1-tracrRNA-crRNA complex, we evaluated whether a single sgRNA could replace the tracrRNA-crRNA complex. Four sgRNA structures were designed to replace the tracrRNA-crRNA complex (Fig. S1), and we estimated their effects on the *trans*-cleavage activity of Cas12c1 (Fig. 1). The results indicated that the fluorescence signals induced by all sgRNAs were significantly higher than those induced by the tracrRNA-crRNA complex. In addition, the sgRNA4 produced the highest fluorescence signal ($p\text{-value} < 0.0001$), and the sgRNA4 structure was used in the following arrays (Fig. 1B). Previous studies verified that Cas12a and Cas12b had different biases on different homopolymeric ssDNA reporters [22,23], and we also estimated the preferences of Cas12c1 on four homopolymeric ssDNA reporters (Table S1). Our results illustrated that Cas12c1 preferred ployT and polyA, rather than polyG and polyC (Fig. 1C). Further, we evaluated the effects of different reaction buffers on the ssDNA *trans*-cleavage activity of Cas12c1 and found that Cas12c1 exhibited the highest *trans*-cleavage activity in Buffer 1 and 3 (Fig. 1D and Table S2). Moreover, we evaluated the effect of spacer length on the *trans*-cleavage activity of Cas12c1 using two targets (HPV16-T1 and T1 sites), and the results showed that the best spacer length is 17 or 18 (Figs. 1E and S2). These results proved that we could reconstruct the ssDNA *trans*-cleavage activity of Cas12c in vitro using the corresponding tracrRNA-crRNA complex or sgRNA.

3.2. Estimation for the sensitivity and specificity of Cas12c-DETECTOR

The sensitivity constrains the practicality and clinical diagnosis of nucleic acid detection platforms [5,22]. Hence, we used two dsDNA activators (HPV16-T1 and T1 sites) to estimate the sensitivity of Cas12c-DETECTOR by setting a series of concentrations of the dsDNA activators (Fig. 2A). Without pre-amplifying the dsDNA activator, Cas12c1 could not induce a detectable fluorescence signal when the activator concentrations were lower than that of 0.23 pM (Fig. 2A), and the corresponding concentration of Cas12a was 3.9 nM (Fig. 2B). Those results indicated that Cas12c1 was more sensitive than Cas12a. Further, we employed the same two dsDNA activators to examine the specificity of Cas12c-DETECTOR by setting a series of single-base mismatches at different positions of the spacer (Figs. 2C and S3). Our results illustrated that the single-base mismatch in the PAM position and mismatches at the distant region within the spacer significantly depressed the *trans*-cleavage activity of Cas12c1, especially the mismatches spanning from 7 to 13 (referred as seed region), indicating that Cas12c1 had high specificity for dsDNA detection (Fig. 2C). Next, we used three sites (APC, HPV16, and HPV18 sites) to compare the specificity of Cas12c1 and Cas12a (Fig. 2D and E). We first examined whether Cas12c1 and Cas12a could be used to identify the SNP in the human *APC* gene (1262G > A) (Fig. 2D and E). Our results indicated that Cas12c1 clearly distinguished the G and A mutation in the *APC* gene (Fig. 2D). In contrast, Cas12a could not identify the 1262G > A (Fig. 2E). Similar results were retained for HPV16 and HPV18 sites (Fig. 2D and E). Those results indicated that Cas12c1 had higher specificity than Cas12a. In total, Cas12c-DETECTOR is a new sensitive and specific nucleic acid detection platform.

3.3. Applications of Cas12c-DETECTOR for nucleic acid detection

We first applied the Cas12c-DETECTOR for the detection of human pathogenic microorganisms. The pandemic caused by the virus CoVID2019 seriously threatened personal and property safety. The accurate clinical diagnosis of the CoVID2019 is the critical step for controlling the pandemic [24]. The E (envelope) gene and the N (nucleoprotein) gene of different beta-coronaviruses (including the CoVID2019 and SARS/Bat-CoV) that were the target genes used for the CoVID2019 identification employed by the procedure of World Health Organization (WHO) diagnosis assay (Table S3) [24]. We synthesized fragments of E and N genes to investigate whether Cas12c-DETECTOR could be applied for the specific detection of the CoVID2019. Next, we designed four and two sgRNAs targeting the N and E genes, respectively (Fig. 3A and B). The N-T1 and N-T2 sgRNA were designed to detect the CoVID2019 N gene, and N-T3 and N-T4 sgRNA were designed to detect the SARS/Bat-CoV N gene (Fig. 3A). The results demonstrated that all four sgRNAs targeting the N gene could distinguish fragments of the two CoVs (CoVID2019 and SARS/Bat-CoV) (Fig. 3A). For sgRNAs targeting the E gene, the *E*-T1 sgRNA was designed to detect both CoVID2019 and SARS/Bat-CoV, and the E-T2 sgRNA was applied to distinguish the two CoVs (Fig. 3B). As expected, E-T1 could detect the fragment of the two CoVs, and E-T2 could specifically detect the fragment of CoVID2019 (Fig. 3B). Therefore, we could infer that Cas12c coupling with the reverse transcription and amplification could be applied for accurate clinical diagnosis of CoVID2019. Then, we applied Cas12c-DETECTOR for the identification of CoVID2019 from clinical samples. Since the lack of clinical samples, we used the contrived samples containing the pseudovirus of CoVID2019 and the rhino pharynx swab collected from the healthy person to stimulate the clinical sample. After the pre-

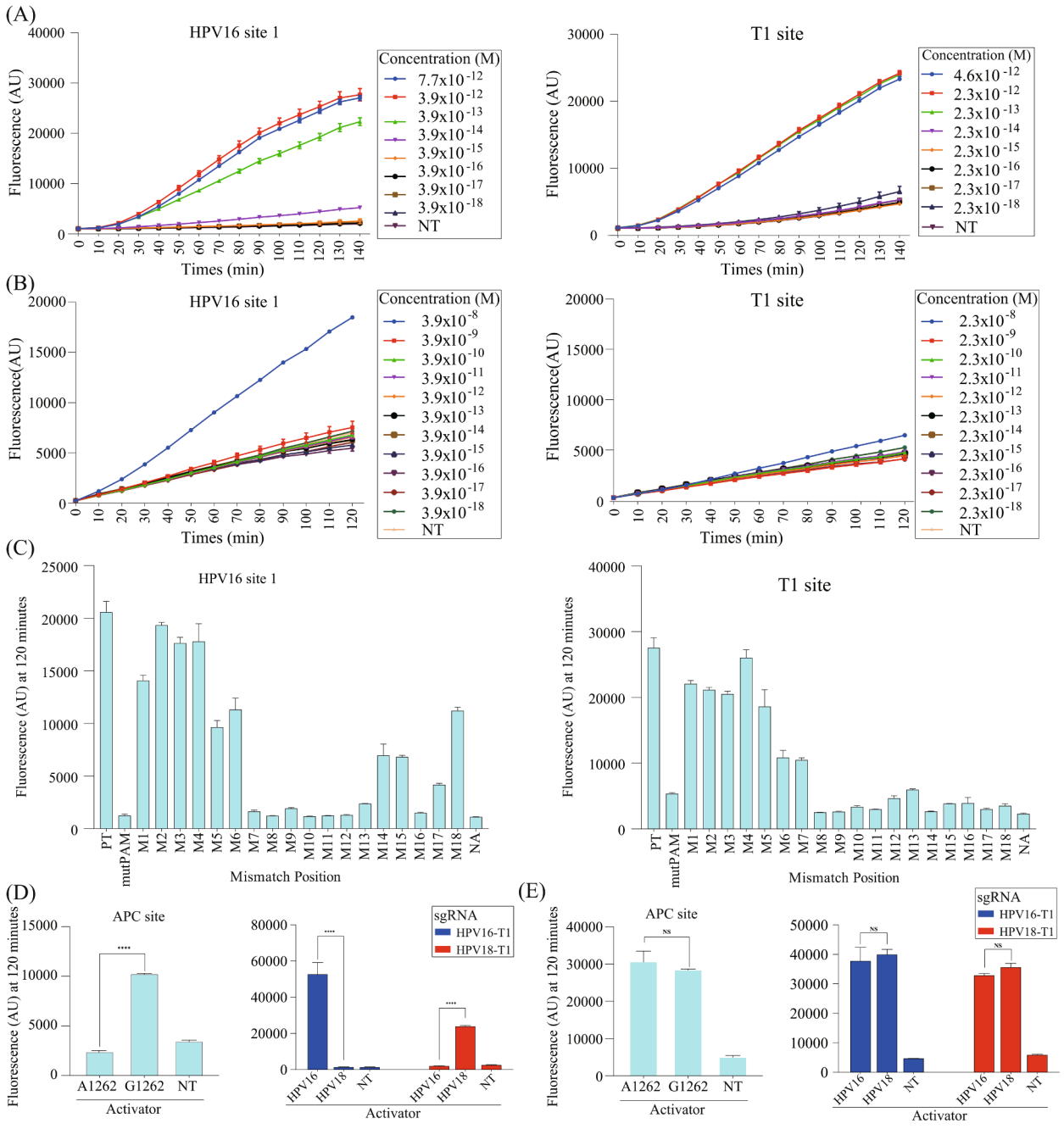


Fig. 2. Sensitivity and specificity of Cas12c-DETECTOR. (A-B) The *trans*-cleavage activity of Cas12c1 and Cas12a incubated with respective sgRNAs targeting the HPV16 and T1 dsDNA activators at different concentrations. Error bars indicate standard errors of the mean (s.e.m.)., n = 3. NT, no-targets. (A) Cas12c1; (B) Cas12a. (C) The *trans*-cleavage activity of Cas12c1 using the HPV16 and T1 dsDNA activators with a single-base mismatch at different spacer positions. (C—D) The fluorescence density induced by the Cas12c1 and Cas12a using *APC*, HPV16 and HPV18 sites after 120 min. Error bars indicate s.e.m., n = 3. The two-tailed Student's *t*-test is used for significance analysis. $*P < 0.05$; $**P < 0.01$; $***P < 0.001$; $****P < 0.0001$; (C) Cas12c1; (D) Cas12a.

amplification using RT-LAMP (Table S4) and the Cas12c-DETECTOR arrays with the E-T2 sgRNA, the fluorescence signal of the mixed sample was significantly higher than that of the unmixed sample and the control, indicating that Cas12c-DETECTOR could be employed for the specific clinical diagnosis of CoVID2019 (Fig. 3C).

The mutant strains of CoVID2019 caused the second wave of the CoVID2019 outbreak [28]. The D614G mutation caused by an A-to-G substitution in the *spike* gene of CoVID2019 enhanced the transmission capacity of CoVID2019, and the identification of this mutation was also crucial for controlling the pandemic [28]. We designed four sgRNAs targeting the *spike* gene to identify the D614G mutation, and the results show that three out of the four sgRNAs could identify this mutation (Figs. 3D and S4). These results indicated that Cas12c-DETECTOR could be used for the accurate and specific identification of CoVID2019 and mutations.

Moreover, we applied Cas12c-DETECTOR to examine plant pathogens causing disasters for the agricultural economy. Kiwifruit bacterial canker disease caused by the *Pseudomonas syringae* pv. *actinidiae* (Psa) is a disaster for the kiwifruit industry [29]. We designed three sgRNAs targeting the *HopZ5* gene, which is the specific *vir* gene of Psa [30]. We found that two out of three sgRNAs induced significantly enhanced fluorescence signals compared to the control, and HopZ5-T2 induced the highest fluorescence using the amplified products of the *HopZ5* gene (Fig. 3E). We further randomly selected ten targets of the HopZ5 gene to

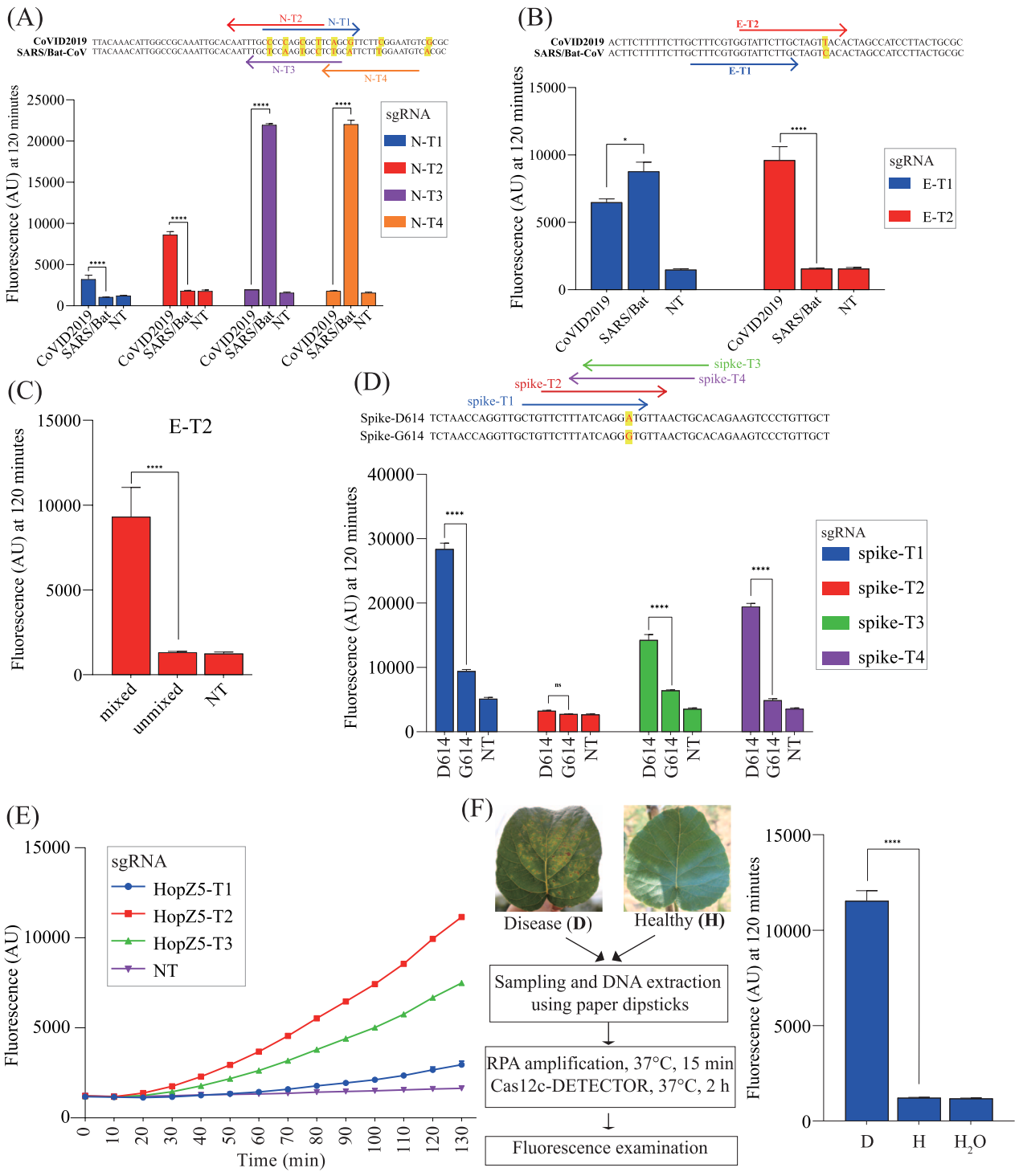


Fig. 3. Wide applications of the Cas12c-DETECTOR. (A) The CoVID2019 and SARS/Bat-CoV identification using Cas12c-DETECTOR with sgRNAs targeting the N gene. (Upper) the sequence variants for the N gene of CoVID2019 and SARS/Bat-CoV and the corresponding sgRNA targets. The yellow rectangle indicated the variations. (Lower) the fluorescence signals for Cas12c-DETECTOR arrays with corresponding sgRNAs at 120 min. (B) The CoVID2019 and SARS/Bat-CoV identification using Cas12c-DETECTOR with sgRNAs targeting the E gene. (Upper) the sequence variants for the E gene of CoVID2019 and SARS/Bat-CoV and the corresponding sgRNA targets. The yellow rectangle indicated the SNP variation. (Lower) the fluorescence signals for Cas12c-DETECTOR arrays with corresponding sgRNAs at 120 min. (C) The detection of CoVID2019 using the contrived samples. Mixed, the contrived sample containing the nasopharynx sample and 50 copies of pseudovirus of CoVID2019; unmixed, the contrived sample just containing the nasopharynx sample; NT, no-target. (D) The distinguish between different lines of CoVID2019 using the SNP variation of the *spike* gene. (Upper) the sequence variants for the *spike* gene of different CoVID2019 lines and the corresponding sgRNA targets. The yellow rectangle indicated the SNP variation. (Lower) the fluorescence signals for Cas12c-DETECTOR arrays with corresponding sgRNAs at 120 min. (E) Fluorescence timecourses for the Cas12c-DETECTOR with sgRNAs targeting the HopZ5 gene of Psa. NT, no-targets. (F) the Psa identification using Cas12c-DETECTOR with HopZ5-T2 sgRNA and RPA from disease and healthy leaves. (Left) the schematic illumination for the Psa identification. (Right) the fluorescence signals for Cas12c-DETECTOR arrays with corresponding sgRNAs at 120 min. For all experiments, error bars indicate s.e.m., n = 3. The two-tailed Student's *t*-test is used for significance analysis. $^{*}P < 0.05$; $^{**}P < 0.01$; $^{***}P < 0.001$; $^{****}P < 0.0001$. NT, no-targets. (For interpretation of the references to colour in this figure legend, the reader is referred to the web version of this article.)

verify the robustness of Cas12c. Our results suggested that eight out of ten targets showed highly efficient and specific identification of the HopZ5 gene (Fig. S5). Next, we test whether Cas12c-DETECTOR coupling with recombinase polymerase amplification (RPA) could be used for Psa identification from healthy and diseased leaves using the HopZ5-T2 target (Fig. 3F). Compared to the fluorescence signal for the healthy leaf, the fluorescence signal for the diseased leaf was significantly enhanced, indicating that Cas12c-DETECTOR coupling with RPA could be applied for the precise identification of Psa (*p-value* < 0.0001) (Fig. 3F). In order to further verify the performance of Cas12c-DETECTOR in actual samples, we collected 44 kiwifruit leaf samples from different kiwifruit orchards for the kiwifruit bacterial canker disease identification using Cas12c-DETECTOR coupling with HopZ5-T2 target. Our results showed that the fluorescence signals of ten samples were similar to the negative control (NT), suggesting the absence of Psa in those ten samples (Fig. S6). While the other 34 samples harbored significantly enhanced fluorescence signals indicating that those samples contained Psa (Fig. S6). The above results indicated that Cas12c-DETECTOR combined with RT-LAMP or RPA could be applied for the specific identification of the human pathogen, plant pathogen, and SNP.

3.4. Visible readout of the Cas12c-DETECTOR

We developed two visualization methods to present the results of Cas12c-DETECTOR to simplify the procedure for presenting the results of Cas12c-DETECTOR. We firstly adapted the lateral flow strip (LFS) to the Cas12c-based DNA detection platform (Fig. 4A). We applied the Cas12c-LFS method to distinguish HPV16, HPV18, SARS-CoV2019, and SARS/Bat-CoV. Our results verified that Cas12c-LFS coupling with the corresponding sgRNAs (HPV16-T1 for HPV and E-T2 for SARS-CoV) could successfully identify HPV16 and SARS-CoV2019 with the appearance of a test line (Fig. 4B). Next, we tested whether the Cas12c-LFS method could be used to identify SNPs. The results indicated that the Cas12c-LFS method specifically identified the SNP in the *spike* gene of SARS-CoV2019 using the *spike*-T1 sgRNA (Fig. 4C). The above results indicated that the Cas12c-LFS method could visually detect DNA and

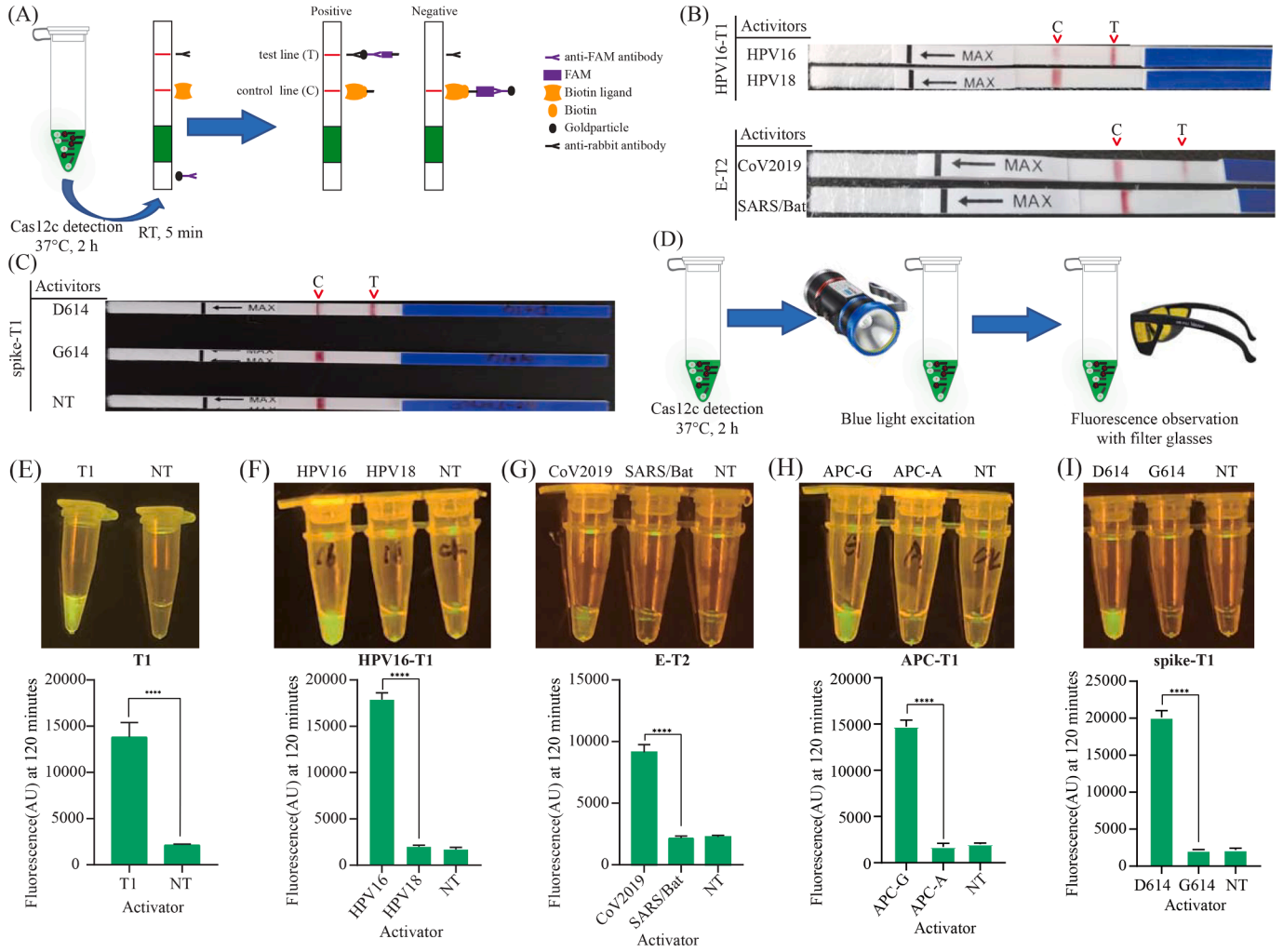


Fig. 4. Visible detection of the Cas12c-DETECTOR. (A) The schematic illumination for the visual detection using Cas12c-DETECTOR and lateral flow strip (Cas12c-LFS) arrays. (B) The visual readout for the identification of HPV16-HPV18 and CoVID2019-SARS/Bat-CoV. (Upper) the result for the identification of HPV16-HPV18. (Lower) the result for the identification of CoVID2019-SARS/Bat-CoV. C, the control line; T, the test line. (C) The visual readout for the identification of SNPs of the *spike* gene. C, the control line; T, the test line. (D) The schematic illumination for the visual detection using Cas12c-DETECTOR and the visual fluorescence detection (Cas12c-VFD) arrays. (E–I) The visual readout of the Cas12c-VFD for different applications. (Upper) visual fluorescence readout under blue light, photographed by digital camera. (Lower) the fluorescence signals for Cas12c-VFD arrays with corresponding sgRNAs at 120 min. Error bars indicate s.e.m., n = 3. The two-tailed Student's t-test is used for significance analysis. **P* < 0.05; ***P* < 0.01; ****P* < 0.001; ****P < 0.0001. NT, no-targets. (E) The result for the identification of the T1 target. (F) The result for the identification of the HPV16 and HPV18. (G) The result for the detection of the CoVID2019 and SARS/Bat-CoV. (H) The result for the detection of the SNP site in the *APC* gene. (I) The result for the detection of the SNP site in the *spike* gene. (For interpretation of the references to colour in this figure legend, the reader is referred to the web version of this article.)

accurate identification of the SNP.

Considering the cost and enormous demands of LFS, we used a visual fluorescence detection (VFD) method to replace the Cas12c-LFP method (Fig. 4D). Cas12c-VFD only needed a blue-light lamp and a yellow filter glass, both of which are low-cost and recyclable, and the results can be interpreted based on the green fluorescence in a reaction solution. We initially tested whether Cas12c-VFD could identify the T1 target (Fig. 4E). Compared to a control tube, the tube containing the T1 dsDNA activator emitted visible green fluorescence, indicating that the Cas12c-VFD method could be applied for rapid DNA detection and fluorescence intensities of those two tubes showed significant differences (Fig. 4E). Additionally, Cas12c-VFD could also be used to distinguish HPV16 from HPV18 and SARS-CoV2019 from SARS/Bat-CoV (Fig. 4F and G). Finally, we tested whether Cas12c-VFD could be applied for SNP identification. SNPs of human *APC* and CoV2019 *spike* genes could be identified successfully by Cas12c-VFD (Fig. 4H and I). The above results indicated that the Cas12c-DETECTOR coupling with LFS or VFD method could be used for visual and fast nucleic acid detection.

4. Discussion

CRISPR/Cas system has been reconstructed for a revolutionary targeted genome modification platform and nucleic acid detection tool [2]. Restricted by the PAM requirement, specificity, and efficiency, more Cas proteins need to be characterized and adapted for genome editing and other applications [4]. The RNA-guided DNA interference activity and ssDNA *trans*-cleavage activity of Cas12c have not been reconstructed in vitro, limiting developments of Cas12c-based platforms [25]. In this study, we reconstructed the ssDNA *trans*-cleavage activity of Cas12c in vitro and developed a highly sensitive and specific Cas12c-mediated nucleic acid detection platform employing its ssDNA *trans*-cleavage activity.

In this study, we first reconstructed the ssDNA *trans*-cleavage activity of Cas12c1 using the tracrRNA-crRNA complex (Fig. 1B). Next, we found that the sgRNA could replace the tracrRNA-crRNA complex (Fig. 1B). We also estimated the ssDNA reporter preference of Cas12c1, and our results illustrated that Cas12c1 preferred ployT and polyA, which was consistent with Cas12a and Cas12b [21–23]. We further optimized the reaction buffer for Cas12c1, and the ssDNA *trans*-cleavage activity of Cas12c1 was significantly affected by the reaction buffer (Fig. 1D). The effect of spacer length on the ssDNA *trans*-cleavage activity of Cas12c1was investigated, and the best spacer length was 17 or 18, which was shorter than that for Cas12a and Cas12b [21–23]. These results indicated that Cas12c was different from Cas12a and Cas12b for some characters.

We also characterized mismatch tolerance of Cas12c1, and our results indicated that Cas12c1 was extremely sensitive to single-base mismatches at the distal region of PAM sequence (Fig. 2C), which was different from Cas12a and Cas12b [21–23]. Those results would enhance the specificity for Cas12c-based nucleic acid detection. By comparing the FQ-based reporter results of Cas12a and Cas12c1 for three targets, Cas12c1 showed higher specificity than Cas12a for nucleic acid detection (Fig. 2D and E). We compared the sensitivities of Cas12a and Cas12c for nucleic acid detection using two targets, and the sensitivity of Cas12c1 increased five orders of magnitude compared to Cas12a (Fig. 2A and B), indicating that Cas12c1 was more suitable for the detection of low concentration nucleic acid. These results illustrated that Cas12c showed higher sensitivity and specificity for nucleic acid detection.

We further applied Cas12c-DETECTOR for pathogens identification and SNP detection. The Cas12c-DETECTOR was successfully applied to detect CoVID2019 using both synthesized fragments and contrived samples and the SNP mutation in the *spike* gene of CoVID2019. The Cas12c-DETECTOR can also be used for plant pathogen detection, such as the pathogen of kiwifruit bacterial canker disease (Fig. 3E and F). Coupling with the LFS and VFD methods, Cas12c-DETECTOR can be applied for the visual detection of nucleic acid detection. Our results illustrated that Cas12c-DETECTOR could be used for highly sensitive and specific nucleic acid detection in clinical diagnosis and other applications.

5. Conclusions

In summary, we firstly characterized and optimized the sgRNA structure, mismatch tolerance, and reaction buffer of Cas12c1 and developed a new sensitive and specific new nucleic acid detection platform based on the Cas12c1. The Cas12c-DETECTOR was successfully applied to detect CoVID2019 using both synthesized fragments and contrived samples and the SNP mutation in the *spike* gene of CoVID2019. The Cas12c-DETECTOR can also be used for plant pathogen detection and SNP identification. Coupling with the LFS and VFD methods, Cas12c-DETECTOR can be applied for the visual detection of nucleic acid detection. Our results illustrated that Cas12c-DETECTOR could be used for rapid, highly sensitive, and specific nucleic acid detection in clinical diagnosis and other applications.

CRediT authorship contribution statement

All authors have no conflicts of interest to declare.

Declaration of competing interest

All authors have no conflicts of interest to declare.

Data availability

No data was used for the research described in the article.

Acknowledgments

This work was supported by the National Key Research and Development Program of China (2019YFD1000201) and the Chinese Academy of Sciences Strategic Leading Science and Technology Project (XDA24030404).

Appendix A. Supplementary data

Supplementary data to this article can be found online at https://doi.org/10.1016/j.ijbiomac.2021.10.167.

References

[1] R. Barrangou, C. Fremaux, H. Deveau, M. Richards, P. Boyaval, S. Moineau, D. A. Romero, P. Horvath, CRISPR provides acquired resistance against viruses in prokaryotes, Science 315 (2007) 1709–1712.
[2] R. Barrangou, P. Horvath, A decade of discovery: CRISPR functions and applications, Nat. Microbiol. 2 (2017) 1–9.
[3] R. Aman, A. Mahas, M. Mahfouz, Nucleic acid detection using CRISPR/Cas biosensing technologies, ACS Synth. Biol. (2020) 1226–1233.
[4] W.X. Yan, P. Hunnewell, L.E. Alfonse, J.M. Carte, E. Keston-Smith, S. Sothiselvam, A.J. Garrity, S. Chong, K.S. Makarova, E.V. Koonin, D.R. Cheng, D.A. Scott, Functionally diverse type V CRISPR-cas systems, Science 363 (2019) 88–91.
[5] J.S. Gootenberg, O.O. Abudayyeh, M.J. Kellner, J. Joung, J.J. Collins, F. Zhang, Multiplexed and portable nucleic acid detection platform with Cas13, Cas12a and Csm6, Science 360 (2018) 439–444, https://doi.org/10.1126/science.aaq0179.
[6] M. Wang, R. Zhang, J. Li, CRISPR/Cas systems redefine nucleic acid detection: principles and methods, Biosens. Bioelectron. 165 (2020), 112430.
[7] R. Nouri, Z. Tang, M. Dong, T. Liu, A. Kshirsagar, W. Guan, CRISPR-based detection of SARS-CoV-2: a review from sample to result, Biosens. Bioelectron. 178 (2021), 113012.
[8] K. Pardee, A.A. Green, M.K. Takahashi, D. Braff, G. Lambert, J.W. Lee, T. Ferrante, D. Ma, N. Donghia, M. Fan, N.M. Daringer, I. Bosch, D.M. Dudley, D.H. O'Connor, L. Gehrke, J.J. Collins, Rapid, low-cost detection of zika virus using programmable biomolecular components, Cell 165 (2016) 1255–1266.
[9] M. Huang, X. Zhou, H. Wang, D. Xing, Clustered regularly interspaced short palindromic Repeats/Cas9 triggered isothermal amplification for site-specific nucleic acid detection, Anal. Chem. 90 (2018) 2193–2200.

[10] R. Wang, X. Zhao, X. Chen, X. Qiu, G. Qing, H. Zhang, L. Zhang, X. Hu, Z. He, D. Zhong, Y. Wang, Y. Luo, Rolling circular amplification (RCA)-assisted CRISPR/Cas9 cleavage (RACE) for highly specific detection of multiple extracellular vesicle MicroRNAs, Anal. Chem. 92 (2020) 2176–2185.
[11] X. Wang, E. Xiong, T. Tian, M. Cheng, W. Lin, H. Wang, G. Zhang, J. Sun, X. Zhou, Clustered regularly interspaced short palindromic Repeats/Cas9-mediated lateral flow nucleic acid assay, ACS Nano 14 (2020) 2497–2508.
[12] K. Guk, J.O. Keem, S.G. Hwang, H. Kim, T. Kang, E.K. Lim, J. Jung, A facile, rapid and sensitive detection of MRSA using a CRISPR-mediated DNA FISH method, antibody-like dCas9/sgRNA complex, Biosens. Bioelectron. 95 (2017) 67–71.
[13] Y. Zhang, L. Qian, W. Wei, Y. Wang, B. Wang, P. Lin, W. Liu, L. Xu, X. Li, D. Liu, S. Cheng, J. Li, Y. Ye, H. Li, X. Zhang, Y. Dong, X. Zhao, C. Liu, H.M. Zhang, Q. Ouyang, C. Lou, Paired design of dCas9 as a systematic platform for the detection of featured nucleic acid sequences in pathogenic strains, ACS Synth. Biol. 6 (2017) 211–216.
[14] R. Hajian, S. Balderston, T. Tran, T. deBoer, J. Etienne, M. Sandhu, N.A. Wauford, J.Y. Chung, J. Nokes, M. Athaiya, J. Paredes, R. Peytavi, B. Goldsmith, N. Murthy, I.M. Conboy, K. Aran, Detection of unamplified target genes via CRISPR–Cas9 immobilized on a graphene field-effect transistor, Nat. Biomed. Eng. 3 (2019) 427–437.
[15] H. Lee, J. Choi, E. Jeong, S. Baek, H.C. Kim, J.H. Chae, Y. Koh, S.W. Seo, J.S. Kim, S.J. Kim, DCas9-mediated nanoelectrokinetic direct detection of target gene for liquid biopsy, Nano Lett. 18 (2018) 7642–7650.
[16] W. Zhou, L. Hu, L. Ying, Z. Zhao, P.K. Chu, X.F. Yu, A CRISPR–Cas9-triggered strand displacement amplification method for ultrasensitive DNA detection, Nat. Commun. 9 (2018) 1–11.
[17] T. Wang, Y. Liu, H. Sun, B. Yin, B. Ye, An RNA-guided Cas9 Nickase-based method for universal isothermal DNA amplification, Angew. Chem. 131 (2019) 5436–5440.
[18] J.S. Gootenberg, O.O. Abudayyeh, J.W. Lee, P. Essletzbichler, A.J. Dy, J. Joung, V. Verdine, N. Donghia, N.M. Daringer, C.A. Freije, C. Myhrvold, R. P. Bhattacharyya, J. Livny, A. Regev, E.V. Koonin, D.T. Hung, P.C. Sabeti, J. J. Collins, F. Zhang, Nucleic acid detection with CRISPR-Cas13a/C2c2, Science 356 (2017) 438–442.
[19] M.J. Kellner, J.G. Koob, J.S. Gootenberg, O.O. Abudayyeh, F. Zhang, SHERLOCK: nucleic acid detection with CRISPR nucleases, Nat. Protoc. 14 (2019) 2986–3012.
[20] L.B. Harrington, D. Burstein, J.S. Chen, D. Paez-Espino, E. Ma, I.P. Witte, J. C. Cofsky, N.C. Kyrpides, J.F. Banfield, J.A. Doudna, Programmed DNA destruction by miniature CRISPR-Cas14 enzymes, Science (80-.) 362 (2018) 839–842.
[21] S.Y. Li, Q.X. Cheng, X.Y. Li, Z.L. Zhang, S. Gao, R.B. Cao, G.P. Zhao, J. Wang, J. M. Wang, CRISPR-Cas12a-assisted nucleic acid detection, Cell Discov. 4 (2018) 18–21.
[22] J.S. Chen, E. Ma, L.B. Harrington, M. Da Costa, X. Tian, J.M. Palefsky, J.A. Doudna, CRISPR-Cas12a target binding unleashes indiscriminate single-stranded DNase activity, Science 360 (2018) 436–439.
[23] F. Teng, L. Guo, T. Cui, X.G. Wang, K. Xu, Q. Gao, Q. Zhou, W. Li, CDetection: CRISPR-Cas12b-based DNA detection with sub-attomolar sensitivity and single-base specificity, Genome Biol. 20 (2019) 1–7.
[24] J.P. Broughton, X. Deng, G. Yu, C.L. Fasching, V. Servellita, J. Singh, X. Miao, J. A. Streithorst, A. Granados, A. Sotomayor-Gonzalez, K. Zorn, A. Gopez, E. Hsu, W. Gu, S. Miller, C.Y. Pan, H. Guevara, D.A. Wadford, J.S. Chen, C.Y. Chiu, CRISPR–Cas12-based detection of SARS-CoV-2, Nat. Biotechnol. 38 (2020) 870–874.
[25] L.B. Harrington, E. Ma, J.S. Chen, I.P. Witte, D. Gertz, D. Paez-Espino, B. Al-Shayeb, N.C. Kyrpides, D. Burstein, J.F. Banfield, J.A. Doudna, A scoutRNA is required for some type V CRISPR-cas systems, Mol. Cell 79 (2020) 416–424.e5.
[26] D. Burstein, L.B. Harrington, S.C. Strutt, A.J. Probst, K. Anantharaman, B. C. Thomas, J.A. Doudna, J.F. Banfield, New CRISPR-cas systems from uncultivated microbes, Nature 542 (2017) 237–241.
[28] B. Korber, W.M. Fischer, S. Gnanakaran, H. Yoon, J. Theiler, W. Abfalterer, N. Hengartner, E.E. Giorgi, T. Bhattacharya, B. Foley, K.M. Hastie, D.G. Parker, Tracking changes in SARS-CoV-2 spike: evidence that D614G increases infectivity of the COVID-19 virus, Cell 182 (2020) 812–827.e19.
[29] H.C. McCann, L. Li, Y. Liu, D. Li, H. Pan, C. Zhong, E.H.A. Rikkerink, M. D. Templeton, C. Straub, E. Colombi, P.B. Rainey, H. Huang, Origin and evolution of the kiwifruit canker pandemic, Genome Biol. Evol. 9 (2017) 932–944.
[30] H.C. McCann, E.H.A. Rikkerink, F. Bertels, M. Fiers, A. Lu, J. Rees-George, M. T. Andersen, A.P. Gleave, B. Haubold, M.W. Wohlers, D.S. Guttman, P.W. Wang, C. Straub, J. Vanneste, P.B. Rainey, M.D. Templeton, Genomic analysis of the kiwifruit pathogen Pseudomonas syringae pv. actinidiae provides insight into the origins of an emergent plant disease, PLoS Pathog. 9 (2013), e1003503.